

Vladimirs Vorohobovs\*, Mārtiņš Kleinhofs

Riga Technical University, Institute of Aeronautics, Faculty of Mechanical Engineering, Transport and Aeronautics, 6B Ķīpsalas St., Kurzemes rajons, LV-1048, Riga, Latvia  
\*Corresponding author. E-mail: riga2006@inbox.lv

Received (Otrzymano) 7.04.2022

## DEFICIENCY-SURPLUS TRANSITION FUNCTION (DeSuTra) IN SEMI-EMPIRICAL FORMULAS FOR TUMBLING OF FREELY FALLING CARD

A new phenomenological method for composing analytical formulae to describe dynamic systems using the DeSuTra function as a building block is introduced. Based on heuristic considerations, it is possible to write a correct formula with several unknown coefficients. Next, these coefficients are tuned such a way that the result coincides with the experimental data. To illustrate the viability of such a method, a simple but not trivial aerodynamic system was chosen: the autorotation of a rectangular piece of paper that falls in air. Three correction coefficients (diminishers) were introduced to calculate its rotation frequency. Then a simple expression for the Magnus effect and drag force was used. All the obtained formulae were experimentally proved and the coefficients calculated. The conclusions drawn confirm the usefulness of the presented calculation procedure for the design of composites with chaotically distributed reinforcements.

**Keywords:** phenomenology, heuristics, semi-empirical research, tumbling cards, Magnus effect, autorotation, lift force, bifurcation, efficiency reducer, efficiency diminisher, DeSuTra function, singularity

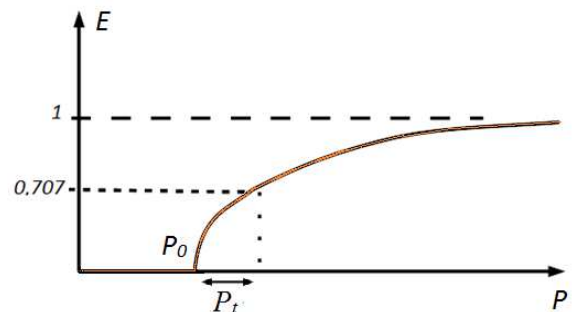
### INTRODUCTION

#### General ideas about Deficiency-Surplus Transition function (DeSuTra function)

In nature, in technology, and in society, there are numerous process which in some ideal circumstances have close to one hundred percent efficiency. However, the lack of “something vital”, which can be measured by parameter  $P$ , leads to a reduction in the efficiency of the process, up to complete cessation if  $P < P_0$ . On the other hand, an overabundance of this “something vital”, does not spoil the process.  $P_0$  is a bifurcation point, described by the general catastrophe theory [1]. A problem also occurs during the design procedure for composite materials containing chaotically distributed reinforcing components or in highly advanced composites containing areas with unpredictable microstructural distortions (for instance stitched fibre reinforced polymer laminates [2]).

An efficiency diminisher is a number between 0 and 1 that shows how much the efficiency of the process is smaller than its possible maximum. The dependence of process efficiency diminisher  $E$  on this vital parameter  $P$  can be visualised by in Figure 1.

The process termination point is a mathematical singular point described by the catastrophe theory. In many systems it looks like a bifurcation point or phase transition point.



where  $P_0$  is the minimal value of  $P$  below which the process stops

Fig. 1. Deficit-Surplus Transition (DeSuTra) function

Therefore, in the vicinity of this point, the behaviour of the system will be described by an analytical function containing a square root. The line here falls sharply. On the other side of the graph at large values of parameter  $P$ , the function tends asymptotically to one. The simplest analytical expression that satisfies these two criteria would be:

$$E_p = \text{Re al} \sqrt{1 - \frac{1}{\frac{P - P_0}{P_t} + 1}} \quad (1)$$

$$\text{if } P > P_0, \text{ or } E_p = 0 \text{ if } P < P_0$$

In this and all further formulae in this text, we assume that if a negative value appears under the square root, the diminisher is simply zero. In other words, we consider only the real part of the result and neglect the imaginary part. This formula includes also another parameter,  $P_t$  – the “thickness” of the transitional zone. It determines that linear expression  $(P - P_0)/P_t$  inside the formula is dimensionless. It can be graphically represented as the difference between the value of the argument at which the function reaches 0.707 and the value of the argument at which the function reaches 0. The goal of our semi empirical method is to find these two coefficients,  $P_0$  and  $P_t$ , experimentally.

Here are some examples of processes which fit this relation:

- Wheat yield as a function of nitrogen in the soil.
- The percentage of germs killed by penicillin as a function of the dose consumed.
- The safe speed of a car as a function of road width.
- Labour productivity as a function of wages.
- The airplane glide ratio as a function of wing length.
- The strength of concrete as function of curing time.

There are certain intuitive rules how to understand if a given process can be described by this formula. First of all, parameter  $P$  must describe something, the absence of which is an obstacle, but not something that acts as the drive of the process or measure of the process. It should also be noted that if in some processes obviously  $P_0 = 0$ , then there is a great probability that the process cannot be described by the analytical expression mentioned above.

Now let us consider what happens if the efficiency depends on two vital parameters –  $P$  and  $R$ . In the simplest case, the two efficiency diminishers,  $E_P$  and  $E_R$ , must be multiplied:  $E = E_P * E_R$ . This is what happens when each diminisher acts sequentially and independently. For example, the efficiency of an electric generator and the efficiency of a high-voltage transformer must simply be multiplied to obtain the total efficiency. In this case, the position of the value of one parameter does not affect the position of the catastrophe point of the other parameter

$$E_{P,R} = E_P * E_R = \sqrt{1 - \frac{1}{\frac{P - P_0}{P_t} + 1}} * \sqrt{1 - \frac{1}{\frac{R - R_0}{R_t} + 1}} \quad (2)$$

The combined effect of non-energy efficiency factors is often just like that. Therefore, this formula can be regarded as the first hypothesis. Moreover, if it works accurately enough, there is no need to look for other more complicated formulas.

## APPLYING THE METHOD TO TUMBLING CARDS

The problem of the flight of a rectangle in the air is undoubtedly a classical problem. Scientists have repeatedly returned to this task [3-8]. It is the most inexpen-

sive object to illustrate the acceptability of our mathematical method in aerodynamics. Air moves around this object in such a complex way that is very difficult to devise a three-dimensional direct solution of the Navier-Stokes equations. That is why nobody has yet delivered simple universal analytical formulas for the general case. The movement of tumbling cards has been illustrated with a stroboscopic photo in [9].

To date, despite its seeming simplicity, this task has not yet had any full compact or precise formulae based on real experimental 3D study. There are some good numerical solutions [10], but obtained only in 2D. Many scientists have limited their attention to a disk, simply because its size is characterized by only one number – the diameter. Plus, a disc falls almost vertically downwards, not deviating from the vertical [9, 11-18]. This reduces the total number of experiments by a factor of ten compared to rectangles, which are characterized by two numbers – length and width. Nevertheless, rectangles tumble and fly at an angle to the vertical much more beautifully and remain in the air longer. The study of rectangles provides more opportunities to illustrate our mathematical method. It also needs to be noted that other methods might also be applied to solve the considered problem [19].

## MATERIALS AND METHODS

### Mathematical approach to obtain some reasonable formulae

The flight of thin rectangles in air fully depends on three values:  $W$  – width,  $L$  – length and  $Z$  – the two-dimensional density of the material. If these three values are established, the flight is fully determined. Therefore, the following three values are also determined:  $f$  – rate of tumbling,  $\alpha$  – angle of deviation of falling motion from the vertical, and  $V_d$  – total speed of declining motion. The speed of setting down will be  $V_{down} = V_d * \cos(\alpha)$ .

Hence, three functions objectively exist:  $f(W,L,Z)$ ,  $\alpha(W,L,Z)$ ,  $V_d(W,L,Z)$ , which describe such dependences that can be found experimentally. Thus, our goal will be to find an analytical expression which describes these functions as precisely as possible. The main idea is to identify several factors of influence and analyse their impact one by one. Each factor of influence can be tuned by changing some coefficients. The best values for the coefficients can be found by experiment.

### Dependence of frequency of rotation from total speed

If we attentively look at the stroboscopic photo in Figure 2, it is clear that the maximal rotating rate cannot exceed a certain value because its upper edge cannot move backwards relative to air. If this maximum is achieved, then the angular frequency of rotation will be:

$$f_{\max} = \frac{V_l}{W} C_f \tag{3}$$

Here  $V_l$  is speed in the tilted direction, and  $W$  – width of the rectangle and  $C_f$  – an unknown universal coefficient –  $C_f \approx 2/\pi$ .

Nonetheless the real frequency will be reduced by three efficiency diminishers:  $E_{Re}$ ,  $E_l$ ,  $E_A$ . According to our working hypothesis, these diminishers are not cumulative, that is why:

$$f_{\max} = \frac{V_l}{W} C_f E_{Re} E_l E_A \tag{4}$$

This hypothesis looks to be very reasonable, but of course our phenomenological method is not strictly mathematical proof. Only an experiment can be the criteria for such non trivial systems. The experiments described by other authors in [14] and in [20] show that the influence of two factors: the Reynolds number and the inertia of the falling object do not create a remarkable nonlinear cumulative effect. In other words, their combined influence can be described as the multiplication of two independent factors; one of them depends only on the Reynolds number and the other depends only on the inertia of the falling rigid body. Our own experiments show that all other diminishers in the formulae, mentioned above, also act as simple diminishers, without any remarkable nonlinear cumulative effect.

**Diminisher  $E_{Re}$**

This is the efficiency diminisher which depends on the viscosity of the air. It is logical to measure the speed of the centre of the strip in Reynolds units and make it dimensionless on the basis of Reynolds’ law of similarity. Therefore, we use  $\frac{V_l \rho W}{\eta}$  instead of the speed.

Thus, using our general theory (1) we obtain:

$$E_{Re} = \sqrt{1 - \frac{1}{\frac{V_l \rho W}{\eta} - Re_0} \frac{\eta}{Re_l} + 1}} \tag{5}$$

at  $\frac{V_l \rho W}{\eta} > Re_0$  otherwise  $B = 0$

where:  $\rho$  – density of the air,  $\eta$  – viscosity,  $W$  – width of the rectangle.  $Re_0$  and  $Re_l$  are dimensionless parameters, which will be found by experiment later.

**Diminisher  $E_l$**

This is the efficiency diminisher which depends on the length of the rectangular strip. Hence, it describes the energy losses on the ends of the strips – boundary

effect. Two-dimensional models are based on the assumption that an rectangle can be made arbitrarily long in the horizontal direction. The easiest way to take in to account the third dimension is to introduce Boundary Factor  $E_l$ , which takes in to consideration motion disrupted by the boundary effect when two ends come too close to each other. This effect is a reason why the problem is sufficiently three-dimensional, and cannot be correctly described as a two-dimensional problem. Diminisher  $E_l$  is a DeSuTra function of ratio  $l = L/W$

$$E_l = \sqrt{1 - \frac{1}{\frac{\frac{L}{W} - l_0}{l_t} + 1}} \tag{6}$$

where  $l_0$  and  $l_t$  are coefficients which determine the rate of this dependence.

$E$  increases asymptotically to its maximal value 1, at  $L/W \gg 1$  when the influence of the edges becomes negligible and motion becomes two-dimensional. In practice,  $L/W$  cannot be less than 1 because otherwise the length and width will be reversed during flight due to instability. However, even a square tumbles quite well. This means that singularity  $l_0$  lies somewhere between 0 and 1, but to find it using a simple rectangle is impossible because of instability – a permutation between the length and width. Finding the point of singularity is only possible by testing special models with stabilization. It was done using double connected rectangles.



Fig. 2. Two rectangles are connected to avoid permutation between  $L$  and  $W$

**Diminisher  $E_A$**

This is efficiency diminisher is determined by comparing the inertial mass of air involved in motion, and the inertial mass of the rectangular itself. The first one is about  $W^2 L \rho$ , and the second is precisely  $W L Z$ , where  $Z$  is the two-dimensional density of thin material  $Z = (\theta - \rho) d$ . Thus, it describes the inertial losses on each turn.

That means that dimensionless parameter  $A = Z/(W\rho)$  determines the situation. It was remarked during the experiments that if  $Z/(W\rho) < A_0 \approx 0.7$ , then the motion becomes chaotic and no smooth tumbling can be observed. In other words, the rectangle must be heavier than the air involved in aerodynamic motion, otherwise the air takes away too much energy from rotation.

Therefore, one more factor should be added to the expression for the rotation frequency:

$$E_A = \sqrt{1 - \frac{1}{\frac{Z}{W\rho} - A_0 + \frac{\eta}{\text{Re}_t} + 1}} \quad (7)$$

This hindering factor is stronger in water than in air. By putting all three diminishers together, it is possible to obtain for rotating frequency  $f$ :

$$f = \frac{V_f}{W} \cdot C_f \cdot \sqrt{1 - \frac{1}{\frac{V_f \rho W}{\eta} - \text{Re}_0 + \frac{\eta}{\text{Re}_t} + 1}} \cdot \sqrt{1 - \frac{1}{\frac{L}{W} - l_0 + \frac{\eta}{\text{Re}_t} + 1}} \cdot \sqrt{\frac{1}{\frac{Z}{W\rho} - A_0 + \frac{\eta}{\text{Re}_t} + 1}} \quad (8)$$

Please remark that  $\text{Re}_0$ ,  $l_0$ ,  $A_0$  are transition points between tumbling and fluttering or the steady descent of falling cards. See [21-23].

**Use of traditional formula for frontal resistance**

Frontal resistance (drag)  $F_D$  can be taken as usual:

$$F_D = C_D L W \rho V_f^2 \quad (9)$$

$C_D$  is a dimensionless parameter, which will be found by experiment later.

**Use of traditional formula for Magnus effect**

Nevertheless, to evaluate the force in the direction perpendicular to motion, we should compare this object with a rotating cylinder, which experiences the Magnus effect. It is known, that the Magnus perpendicular force is equal to  $F_M = L V_f \rho \Gamma$ , where  $\Gamma$  is the circulation of speed for a cylinder with radius  $r$   $\Gamma = (2\pi r)^2 f$ , and thus  $F_M = (2\pi r)^2 f L V_f \rho$ . On the other hand, for the specific geometry of a tumbling rectangle, some other coefficients can appear here. Hence, we can assume that  $F_M = C_M \cdot f \cdot W^2 L V_f \rho$ , where  $C_M$  is an unknown coefficient, which depends on geometry but must be the same for geometrically similar rectangles.

Therefore, the Magnus force is:

$$F_M = W L V_f^2 \rho C_M \cdot C_f \cdot \sqrt{1 - \frac{1}{\frac{V_f \rho W}{\eta} - \text{Re}_0 + \frac{\eta}{\text{Re}_t} + 1}} \cdot \sqrt{1 - \frac{1}{\frac{L}{W} - l_0 + \frac{\eta}{\text{Re}_t} + 1}} \cdot \sqrt{\frac{1}{\frac{Z}{W\rho} - A_0 + \frac{\eta}{\text{Re}_t} + 1}} \quad (10)$$

**Application of Newton's laws to this system**

The vector sum of drag force and Magnus force should be compensated by gravity force.  $WLZg$ , where

$g = 9.8 \text{ m/s}^2$ , and  $d$  is the thickness of the rectangle. If  $\alpha$  is an angle between the inclined direction of motion and the vertical, then the force equilibrium in the vertical direction requires:

$$WLZg = F_D \cos(\alpha) + F_M \sin(\alpha) \quad (11)$$

However, the force equilibrium in the horizontal direction requires:

$$F_M \cos(\alpha) = F_D \sin(\alpha) \quad (12)$$

which means:

$$\text{tg}(\alpha) = F_M / F_D \quad (13)$$

$$\text{tg}(\alpha) = \frac{C_M}{C_D} \cdot C_f \cdot \sqrt{1 - \frac{1}{\frac{V_f \rho W}{\eta} - \text{Re}_0 + \frac{\eta}{\text{Re}_t} + 1}} \cdot \sqrt{1 - \frac{1}{\frac{L}{W} - l_0 + \frac{\eta}{\text{Re}_t} + 1}} \cdot \sqrt{\frac{1}{\frac{Z}{W\rho} - A_0 + \frac{\eta}{\text{Re}_t} + 1}} \quad (14)$$

The expression in brackets here will not depend on size but only on form. The expression under the square root depends only on the width. Now let us assemble all the previous formulae together. Thus, we get:

$$F_D = (WLZg) \cos(\alpha) = \frac{WLZg}{\sqrt{1 + \text{tg}^2(\alpha)}} \quad (15)$$

$$C_D L W \rho V_f^2 = \frac{WLZg}{\sqrt{1 + \text{tg}^2(\alpha)}} \quad (16)$$

From here we will obtain the expression for speed:

$$V_f = \frac{1}{\sqrt{C_D}} \sqrt{\frac{Zg}{\rho}} \cdot \frac{1}{\sqrt[4]{1 + \text{tg}^2(\alpha)}} \quad (17)$$

but for falling speed

$$V_{down} = \frac{1}{\sqrt{C_D}} \sqrt{\frac{Zg}{\rho}} \left/ \left( \sqrt[4]{1 + \text{tg}^2(\alpha)} \right)^3 \right. \quad (18)$$

At  $\alpha \rightarrow 0$  – this expression coincides with the result received by Changqui in [24]  $V_{down} = K \sqrt{\frac{(\theta - \rho)gd}{\rho}}$ .

where  $K = \frac{1}{\sqrt{C_D}}$ ,  $Z = (\theta - \rho)d$ . Actually, all the de-

pendences on the sizes of the rectangle lie only in the expression for  $\text{tg}(\alpha)$ .

It is interesting to remark that squares ( $L = W$ ) cut from the same paper fall approximately at the same speed. This occurs because if  $L = W$ , spoiling boundary factor  $E_l$  goes down to  $1/2$ , and that is why  $\text{tg}(\alpha)$  is much smaller than 1 and  $\frac{1}{\sqrt[4]{1 + \text{tg}^2(\alpha)}} \approx 1$ .

Nonetheless, it is not the case for elongated rectangles ( $L > 2W$ ), which move and rotate with greater effectiveness -  $\text{tg}(\alpha) > 0.8$ . For them, the speed of descent depends on size and on form, which is very remarkable. These equations are easily solved by the method of successive approximations. First we have to consider  $\alpha = 0$ , then solve (17), then (14) and receive a new value for  $\alpha > 0$ , then (17) again and receive new value for  $V$ , then (13) again. It is usually sufficient to make two iterations.

After finding  $V$  and  $\alpha$ , the rotation rate can be easily calculated by (8) and falling speed by (18).

managed to measure the rotational speed of the tumbling of a small paper card. The formula proposed above for the period of tumbling of a thin card was fully confirmed in the range of parameters in which the falling was periodic and the axis of rotation was horizontal.

TABLE 1. Coefficients determined by processing experimental data

$\eta/\rho$	$g$	$\rho$	$C_f$	$C_M$	$C_D$	$Re_0$	$Ret$	$l_0$	$l_t$	$A_0$	$A_t$
0,0000148	9.8	1.2	0.3	4	0.5	100	700	0.2	0.2	0.9	0.7

## RESULTS AND DISCUSSION

### Experimental part

In order to determine the rotational speed of the falling card, a camera with fast shooting of 240 frames per second was used. With this camera, we

The smallest paper rectangle that we were able to cut from paper and to observe its falling speed in the air had  $W = 2.5$  mm. The largest rectangle was a plastic sheet, 490x170x2 mm in size. They correspond to Reynolds numbers from 170 to 24000.

TABLE 2. Comparison of experimental data and theoretical predictions

Parameters			Experiment						Theory		
Surface density $Z$	Width $W$	Length $L$	Rate of tumbling $f$	error	Down speed	error	$\text{tg}(\alpha)$	error	Rate of tumbling $f$	Down speed	$\text{tg}(\alpha)$
0.068	0.0025	0.0025	26.8	1.6					32.1428	0.79852	0.6691
0.068	0.005	0.005	18.1	1.3					23.3812	0.59222	1.0754
0.068	0.01	0.01	10.8	2					13.8514	0.4774	1.36907
0.068	0.02	0.02	6.3	2					7.31887	0.43913	1.48766
0.068	0.04	0.04	4	2					3.25166	0.52079	1.24884
0.068	0.08	0.08	unstable						#####	#####	#####
0.046	0.0025	0.0025	21.8	6					21.3294	0.72313	0.52279
0.046	0.0025	0.0075	21.6	5					22.8368	0.70432	0.56467
0.046	0.005	0.015	18.9	2					18.5721	0.50552	1.0258
0.046	0.01	0.03	13.3	1					11.1904	0.40284	1.33336
0.046	0.02	0.06	7.2	1					5.74817	0.38748	1.38768
0.046	0.02	0.06	7.2	2					5.74817	0.38748	1.38768
0.437	0.135	0.44	3	0.2	1.5	0.2	2	0.5	3.25325	0.82616	1.94477
2	0.17	0.492	4.5	0.2	3.7	0.6	1	0.2	5.97558	1.50622	2.21779
0.5	0.11	0.42	4.6	0.2	2.4	0.5	2	0.5	4.42356	0.82365	2.06217
0.154	0.005	0.015	25.6	4	1.1	0.3			42.6491	0.6947	1.41635
0.154	0.01	0.03	21.4	5	2	0.5			24.1571	0.56587	1.71803
0.154	0.02	0.06	11.5	2	1.6	0.5	1	0.2	12.7912	0.50881	1.88502
0.154	0.04	0.12	5.9	0.5	1.5	0.3	0.8	0.2	6.38508	0.51042	1.87993
0.154	0.08	0.24	3.2	0.4	1.2	0.2	0.9	0.2	2.86104	0.62109	1.57805
0.068	0.0025	0.0075	37.1	5					34.2848	0.76898	0.72271
0.068	0.005	0.015	26.3	7	1.3	0	1	0.2	24.7198	0.55539	1.16157
0.068	0.01	0.03	15.9	3	0.9	0.1	2	0.5	14.5802	0.44186	1.47877
0.068	0.02	0.06	8.3	0.3	0.8	0.2	1.2	0.3	7.69341	0.40476	1.60686
0.068	0.04	0.12	4.1	0.5	0.9	0.4	0.9	0.2	3.42829	0.48435	1.3489
0.068	0.08	0.24	Non unstable		1	0.3			#####	#####	#####
0.134	0.015	0.075	15						15.5954	0.49288	1.82475

All values here are in SI.

As a result, we were not able to find a proper precise value for  $Re_0$  because the frequency of our camera frame does not allow this. We can only evaluate approximately that  $Re_0 = 100$ . This is close to the results obtained by Field et al. in [14, 20]. It was proven experimentally that the formulae give correct results for all such different objects. The tumbling of a falling metal plate was also observed in water; nevertheless, because the density of water is much greater, diminisher  $E_A$  mentioned above declines much quicker. Actually, only relatively thick sheets of heavy metal like cuprum or gold coins tumble in water. We did not conduct many experiments in water, but it is possible to find such studies in [25-30]. Our analytical formula fully coincides with their results. Therefore, the above formula was also confirmed for water. Thus, the simplest dependence law between the size of the rectangle, its rotation period and down speed was experimentally proved.

The above conclusions may also contribute to the design of composite materials and multimaterial complex composite structures [31-33]. It may significantly shorten the design process and eliminate a part of preliminary evaluation of the designed structure.

## CONCLUSIONS

Formulae can be used to calculate the frequency and speeds of the tumbling of a falling rectangle. They can be used for optimisation or any other purposes. As can be seen from this study, the same formula describing deceleration due to energy losses was successfully applied three times for three different factors. The deep reason lies in the fact that they are all manifestations of the same phenomenon: the growth of entropy, and the growth of entropy leads to the fact that different objects become almost similar and can be described by similar formulas. This fundamental property of the Universe suggests that the same mathematical formula (1) can become one of the building blocks of the mathematical description of thousands of other objects in which some irreversible processes occur. In aerodynamics, this approach allows us to receive an answer by eliminating the need to solve complex Navier-Stokes equations. This cannot be done without experimentation, but knowledge of the general form of the analytical solution will greatly reduce the number of required experiments.

## REFERENCES

- [1] Zeeman E.C., Catastrophe Theory – Selected Papers 1972-1977, Addison-Wesley, Reading, MA 1977.
- [2] Koziol M., Effect of thread tension on mechanical performance of stitched glass fibre-reinforced polymer laminates – experimental study, *Journal of Composite Materials* 2013, 47, 16, 1919-1930, DOI: 10.1177/0021998312452179.
- [3] Jones M.A., Shelley M.J., Falling cards, *J. Fluid Mech.* 2005, 540, 393-425 DOI: 10.1017/S0022112005005859.
- [4] Mittal R., Seshadri V., Udaykumar H.S., Flutter, tumble and vortex induced autorotation, *Theor. Comput. Fluid Dyn.* 2004, 17(3), 165-170, DOI: 10.1007/s00162-003-0101-5.
- [5] Smith A.M.O., On the motion of a tumbling body, *Journal of the Aeronautical Sciences* 1953, 20, 2, 73-84.
- [6] Smith E.H., Autorotating wings: An experimental investigation, *J. Fluid Mech.* 1971, 50, 513-534, DOI: 10.1017/s0022112071002738.
- [7] Wang W.B., Hu R.F., Xu S.J., Wu Z.N., Influence of aspect ratio on tumbling plates, *Journal of Fluid Mechanics* 2013, DOI: 10.1017/jfm.2013.461.
- [8] Wang Y., Shu C., Teo C.J., Yang L.M., Numerical study on the freely falling plate: Effects of density ratio and thickness-to-length ratio editors-pick, *Physics of Fluids* 2016, 28, 103603, DOI: 10.1063/1.4963242.
- [9] Heisinger L., Coins falling in water 2013, <https://arxiv.org/pdf/1312.2278.pdf>.
- [10] Assemat P., Fabre D., Magnaudet J., The onset of unsteadiness of two-dimensional bodies falling or rising in a viscous fluid: A linear study, *J. Fluid Mech.* 2012, 690, 173-202, DOI: 10.1017/jfm.2011.419.
- [11] Auguste F., Magnaudet J., Fabre D., Falling styles of disks, *J. Fluid Mech.* 2013, 719, 388-405, DOI: 10.1017/jfm.2012.602.
- [12] Chrust M., Bouchet G., Dušek J., Numerical simulation of the dynamics of freely falling discs, *Phys. Fluids* 2013, 25(4), 044102, DOI: 10.1063/1.4799179.
- [13] Lee C.B., Su Z., Zhong H.J., Chen S.Y., Zhou M.D., Wu J.Z., Experimental investigation of freely falling thin disks. Part 2. Transition of three-dimensional motion from zigzag to spiral, *J. Fluid Mech.* 2013, 732, 77-104, DOI: 10.1017/jfm.2013.390.
- [14] Field S.B.M., Klaus M., Moore G., Nori F., Chaotic dynamics of falling disks, *Letters of Nature* 1997, <http://www.nature.com/nature/journal/v388/n6639/full/388252a0.html>.
- [15] Vincent L., Shambaugh W.S., Kanso E., Holes stabilize freely falling coins, *J. Fluid Mech.* 2016, 801, 250-259, DOI: 10.1017/jfm.2016.432.
- [16] Fernando V., Caetano R., Calculation of dynamic behaviour of falling disc or plate in fluid 2010, <https://fenix.tecnico.ulisboa.pt/downloadFile/395142133553/resumo.pdf>.
- [17] Zhong H.J., Lee C.B., Su Z., Chen S.Y., Zhou M.D., Wu J.Z., Experimental investigation of freely falling thin disks. I. The flow structures and Reynolds number effects on the zigzag motion, *J. Fluid Mech.* 2013, 716, 228-250, DOI: 10.1017/jfm.2012.543.
- [18] Zhong H., Chen S.Y., Lee C., Experimental study of freely falling thin disks: Transition from planar zigzag to spiral, *Phys. Fluids* 2011, 23, 011702, DOI: 10.1063/1.3541844.
- [19] Chatys R., Application of the Markov chain theory in estimating the strength of fiber-layered composite structures with regard to manufacturing aspects, *Advances in Science and Technology Research Journal* 2020, 14 (40), 1-8.
- [20] Iversen J.D., Autorotation flat-plate wings: The effect of the moment of inertia, geometry and Reynolds number, *J. Fluid Mech.* 1979, 92, 327-348, DOI: 10.1017/s0022112079000641.
- [21] Andersen A., Pesavento U., Wang Z.J., Analysis of transitions between fluttering, tumbling and steady descent of falling cards, *J. Fluid Mech.* 2005, 541, 91-104, DOI: 10.1017/S0022112005005847.

- [22] Andersen A., Pesavento U., Wang Z. J., Unsteady aerodynamics of fluttering and tumbling plates, *J. Fluid Mech.* 2005, 541, 65-90, DOI: 10.1017/S002211200500594X.
- [23] Belmonte A., Eisenberg H., Moses E., From flutter to tumble: Inertial drag and froude similarity in falling paper, *Phys. Rev. Lett.* 1998, 81(2), 345-348, DOI: 10.1103/physrevlett.81.345.
- [24] Changqui J., Numerical study of unsteady aerodynamic of falling plate, <http://www.math.ust.hk/~makxu/PAPER/CiCP-Jin-Xu.pdf>.
- [25] Bonisch S., Heuveline V., On the numerical simulation of the unsteady free fall of a solid in fluid. I. The Newtonian case, *Comput. Fluids* 2007, 36(9), 1434-1445, DOI: 10.1016/j.compfluid.2007.01.010.
- [26] Ern P., Risso F., Fabre, D., Magnaudet J., Wake-induced oscillatory paths of bodies freely rising or falling in fluids, *Annu. Rev. Fluid Mech.* 2012, 44(44), 97-121, DOI: 10.1146/annurev-fluid-120710-101250.
- [27] Maxwell J.C., Niven W.D., Maxwell J.C., On a particular case of the descent of a heavy body in a resisting medium, Cambridge University Press, 1853.
- [28] Pesavento U., Wang Z.J., Falling Paper: Navier-Stokes solutions, model of fluid forces, and center of mass elevation, *Phys. Rev. Lett.* 2004, 93(14), 144501, DOI: 10.1103/physrevlett.93.144501.
- [29] Field S.B., Klaus M., Moore M.G., Nori F., Chaotic dynamics of falling disks, *Nature* 1997, 388(6639), 252-254 DOI: 10.1038/40817.
- [30] Mahadevan L., Tumbling cards, *Physics Fluid* 1999, <https://www.seas.harvard.edu/softmat/downloads/pre2000-05.pdf>.
- [31] Toroń B., Szperlich P., Koziół M., SbSI composites based on epoxy resin and cellulose for energy harvesting and sensors – the influence of SBSI nanowires conglomeration on piezoelectric properties, *Materials* 2020, 13(4), 902, DOI: 10.3390/ma13040902.
- [32] Chatys, R., Orzechowski, T., Surface extension in layered structures with the use of metal meshes for heat-transfer enhancement, *Mechanics of Composite Materials* 2004, 40(2), 159-168.
- [33] Olesik P., Godzierz M., Koziół M., Preliminary characterization of novel LDPE-Based wear-resistant composite suitable for FDM 3D printing, *Materials* 2019, 12, 2520, DOI: 10.3390/ma12162520.